Year: 2019

Undertakings in 2017 and 2018 in Phojikha as Part of Phase III of the Bhutan-Swiss Archaeology Project

Karma, Tenzin ; Burkart, Ulrich ; Bader, Christian ; Hart, Benjamin ; Keiser, Alex

Undertakings in 2017 und 2018 in Phobjikha as Part of Phase III of the Bhutan-Swiss Archaeology Project

Karma Tenzin, Burkart Ullrich, Christian Bader, Benjamin Hart, Alex Keiser

Different sites in
Gangtey Gewog and Phobji Gewog
Wangdue Phodrang Dzongkhag, Bhutan

Map. No. Bhutan 1 : 50 000 No. 78 i-3
Central coordinates E 90° 11' 11.3", N 27° 27' 35.0"
Average altitude 2900 m above sea level

1. Background Situation

Phobjikha is a vast glacial-formed valley at about 3000 m a.s.l., which descends from Bhutan's East-West Highway a few kilometres before Pele pass, the boundary between western and central Bhutan. From the northernmost to the southernmost settlements, the valley has a length of about 15 km, with villages nestled at the foot of the slope because the valley plain consists of wet marshland (fig. 1).

In autumn 2013, the project team of the Bhutan-Swiss Archaeology Project had already begun to turn their attention to Phobjikha. At Peter Fux's (University of Zurich and Museum Rietberg Zurich) initiative, the archaeologists surveyed the valley, together with Namgyel Tshering, at that time Program Manager, Helvetas Swiss Intercooperation Bhutan (Fux et al. 2014). Near the Ngelung Drechagling Lhakhang nunnery they documented several accumulations of artificial mound structures. Another individually situated large mound exhibited an obvious capped knoll (Fux et al. 2014).

A further visit to the valley in autumn 2014 by Philippe Della Casa (University of Zurich), Peter Fux, Christian Bader, and Namgyel Tshering led to the discovery of more artificial mounds. Some of these in areas being farmed near a village called Kilkhorthang in Phobji Gewog had already been severely damaged by being ploughed (see fig. 6). Due to the promising features and particularly the precarious situation of individual mounds, Phobjikha was subsequently suggested as one of the research priorities for the upcoming Phase III of the Bhutan-Swiss Archaeology Project (Della Casa et al. 2015, p. 170).

2. Prospection and Inventory in Autumn 2017

The brief visits to Phobjikha in 2013 and 2014 had demonstrated that the settlement areas constitute a rich cultural landscape with a wealth of testimony on the centuries-old history of the valley. Since the majority of all the archaeological and architectural

Fig. 1 Phobjikha with Ramsar wetland at the bottom of the valley and settlement areas at the foot of both slopes

1

2

Fig. 2 Geographic location of the Phobjikha Valley in the Wangdue Phodrang Dzongkhag

Fig. 3 Village inhabitant tells about find spot

Fig. 4 Documentation work on a ruin in the forest

Fig. 5 Mound near the village of Damche Lhakhang

Fig. 6 Endangered mound near the village of Kilkhorthang that has been cut through by agrarian ploughing

monuments had not been previously recorded as such, it seemed important to first get an overview of the historical-archaeological sites in the valley. We therefore decided to carry out a landscape prospection in Phobjikha with a systematic field survey and interviews of the village inhabitants (figs. 3–6). The project was intended to be exemplary for future inventories and the targeted results included providing a catalog of find spots with localizations, brief comments, a description, and photographic documentation of the respective find spot. In addition, a classification of each find spot should include an assessment of the degree of preservation, precariousness of the situation, and recommendations for a future cultural site management program.

3

4

5

6

Fig. 7 Inventory 2017, distribution of find spots
A: Artificial Hill; AL: Artificial Landscape;
M: Mound; MW: Menchu Water; S: Structure;
SS: Sacred Site; T: Terrace

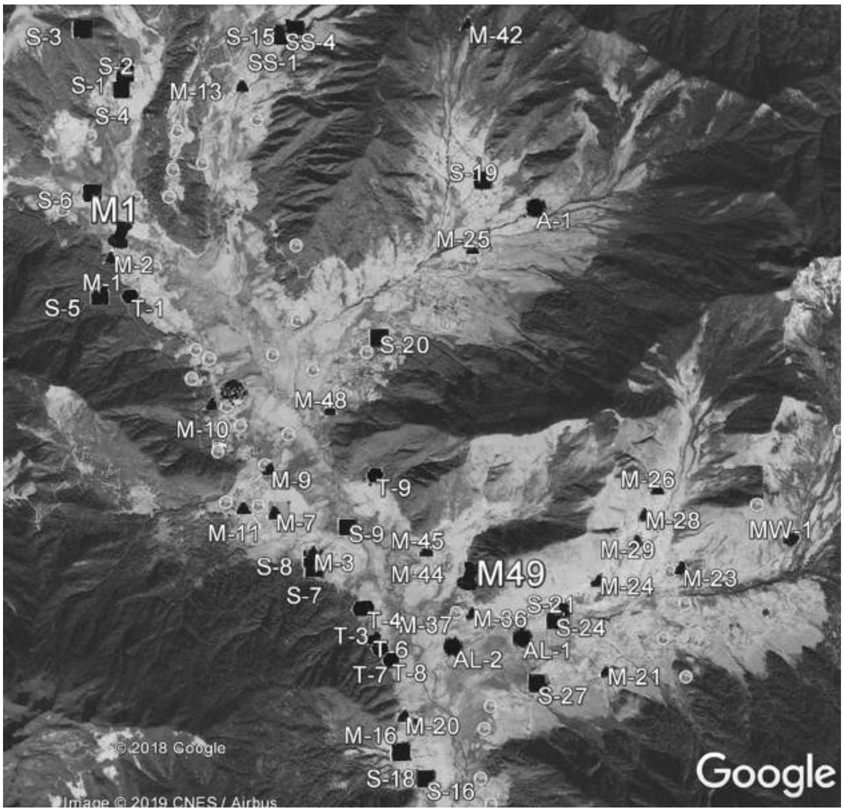

7

For four weeks from 6 November to 1 December, 2017, two groups with four persons each combed through the entire Phobjikha Valley from north to south, searching for artificial changes to the terrain and for buildings. In the process, wherever possible, the older villagers were interviewed and questioned about cultic places, abandoned buildings, or ruins. The two groups were composed as follows:

Group 1: Karma Tenzin, Division for Conservation of Heritage Sites (DCHS), Head of Section for Archaeology; Sonam Gyeltsen, DCHS; Shacha Gyeltsen, Cultural Officer Wangdue Phodrang District; Tashi Dawa, Cultural Officer Trashiyangtse District.

Group 2: Christian Bader, SLSA; Sonam Tenzin, DCHS; Tenzin Wangchuk, DCHS; Pema Wangda, Cultural Officer Samdrup Jongkhar District.

During this month of conducting the inventory, a total of ninety-three find spots were detected and described, of which at least forty-nine were presumed to be burial mounds due to their topographical characteristics (fig. 7). The archaeological find spots were mostly located in the district area of an existing settlement. It can therefore be assumed that most villages have existed for centuries and that they have been settled continuously for a long period.

3. Geophysical Surveys in Spring 2018

After forty-nine artificial mounds had been identified during the inventory in autumn 2017, six mounds that appeared to be particularly interesting were to be scanned in spring 2018 using geophysical survey methods. The aim was to initially acquire data about the manner of construction and inner structure without any excavation and thereby at best to gather indications leading to an interpretation. The work was conducted over two weeks from 26 February to 9 March, 2018. The Mounds M1, M3, M31, M34, M36, and M49 were investigated. On the one hand, Ground Penetrating Radar

Method	Geophysical Surveys		Topographical Surveys		Reference point
Mound	**GPR**	**ERT**	**GNSS**	**Theodolite**	**Fixed Point No.**
M1	57 profiles two areas with a total of 160 m²	3 profiles, 39 electrodes, distance 0.75 m	corners of GPR area, electrode positions stones at surface	topography	13971
M3	41 profiles Area: 18 m × 10 m	17 profiles, 20 electrodes, distance 0.5 m	corners of GPR area	topography, electrode positions	17657
M31	44 profiles Area: 15 m × 11 m	8 profiles, 33 electrodes, distance 0.5 m	corners of GPR area and trench S1 / section	topography, electrode positions	17688
M34	53 profiles Area: 15 m × 12 m		corners of GPR area		
M36	57 profiles Area: 15 m × 14 m		corners of GPR area		
M49	125 profiles Area: 21 m × 31 m		corners of GPR area		

Table 1 Overview of surveys conducted at the Phobjikha Valley mounds

(GPR) and, on the other, Electrical Resistivity Tomography (ERT) were used as methods, both supplemented by topographical surveys at these mounds.

Burkart Ullrich of Eastern Atlas GmbH & Co. KG, Berlin, was enlisted for this work. Assisting him were Benjamin Hart and Alexander Keiser, two masters students in archaeology at the University of Zurich. In addition, under the direction of Karma Tenzin and Christian Bader, the following DCHS staff members supported the project team's work: Sonam Tenzin, Tenzin Wangchuk, Sonam Gyeltsen, Shacha Gyeltsen, and Tashi Dawa.

3.1 Surveyed Mounds in the Phobjikha Valley

The mounds in the Phobjikha Valley vary in terms of their size, elevation, steepness, and degree of preservation. The prominence of isolated mounds differs from that of single mounds that are arranged in rows or groups. The following mounds (table 1) were selected for the geophysical surveys:

Mound M1

Mound M1 is a single standing mound located in the upper north-western part of the valley in the village of Mole in Gangtey Gewog (figs. 8 and 21). There are large stone wall constructions north of the mound. Mound M1 is located in view of the famous Gangteng Monastery, about 1 km northeast across the valley.

Mound M3

Mound M3 is located on the western slope of the central valley in the village of Uesa in Gangtey Gewog (figs. 9 and 22). It is the northernmost mound of a group of several mounds (M3, M4, M5, and M6) with remains of the walls of a building (sites S7 and S8) nearby. A local shrine of the village of Uesa is located about 100 m south-east of Mound M3.

The surveyed Mounds M31, M34, M36, and M49 are grouped among others in the south-eastern part of the Phobjikha Valley at the promontory above the junction of the valley overlooking the confluence of two streams (figs. 10 and 11).

Mound M31

The easternmost mound, M31 (figs. 11 and 23), is capped and located south of a road running east-west and approximately 175 m north-west of the remarkable monumental cone-shaped Mound M32 at the bottom of the valley. A pit is located at the north-

Fig. 8 Mound M1 viewed from the south-east during the GPR survey

Fig. 9 Mound M3 viewed from the flat western part

Fig. 10 Mounds M33 to M35 with M34 in the centre

Fig. 11 Mound M31 with trench S1 viewed from the road

western edge of Mound M31. During the autumn 2018 campaign this pit was expanded into a trench S1 and documented by the archaeological team (fig. 26).

Mound M34

Mound M34 is the central one of a group of three mounds (M33, M34, and M35) arranged in a row from east to west as mentioned previously (Fux et al. 2014, p. 37). The area is covered by prayer flags and is clearly visible from the street (fig. 10).

Mound M36

Mound M36 (figs. 12 and 25) is one in a group of several mounds extending from M36 to M41. This group of mounds is located in a forested part in the east of the fenced area of the Ngelung Drechagling Lhakhang nunnery. During the survey the coordinates of five other mounds were also registered and numbered clockwise around Mound M36. They are mainly recognizable as small elevated hills. However, the mounds in the south of the group do not clearly show a highest point. M40 is located near the remains of a modern building. Mound M41 is about 20 m west of M36 and has a wooden cabin on top.

Mound M49

Mound M49 is a huge capped mound north of the monastery with a clearly visible plateau, the result of recent bulldozing activity (fig. 13)

3.2 Methodology and Equipment used for the Geophysical Surveys

Ground Penetrating Radar (GPR)

The GPR method is based on the propagation of high-frequency electromagnetic waves into the ground. The waves are reflected and refracted by different layers and objects

8

9

10

11

12

13

Fig. 12 Mound M36 in the area of the Ngelung Drechagling Lhakhang nunnery

Fig. 13 View from the road to Mound M49

like stones and walls. The registration of transit time differences and amplitudes of the electromagnetic waves provides information about position, depth, and specific properties of buried objects and layers. Spherical resolution and depth of penetration depend on the GPR antenna's frequency and the electromagnetic properties of the ground. A rule of thumb is that the higher the frequency, the better the spherical resolution, but with falling depth of penetration. For the investigations in the Phobjikha Valley, the GPR system SIR-3000 from GSSI with a 270 MHz antenna and survey wheel was used (figs. 8 and 11).

The propagation conditions of electromagnetic waves are determined by the soil properties. The main factor is the water content since water has a very high dielectric permittivity ε, which causes a strong attenuation of electromagnetic waves. For this reason dry ground offers more favourable conditions for GPR measurements than saturated soils. Another important influence comes from clay minerals. In most cases penetration depth and resolution of GPR measurements in clayey soils are very poor. This is due to the presence of crystallized water bound with clay minerals (Jol 2009).

Actual survey conditions in the Phobjikha Valley were very favourable for GPR surveying. At the end of a very dry season, the ground was parched. Furthermore, the soil, which has been generated from the bedrock formation, contains only a small amount of clay producing a high attenuation of the electromagnetic waves. These conditions meant that significant reflections of up to a two-way transit time of 80 ns could be registered. With a wave velocity of 0.8 m/ns, obtained from the curvature of diffraction hyperbolas, a depth penetration of up to 3.2 m could be reached. Table 2 lists the technical data of the GPR survey equipment used.

The specific surface of the mounds results in the unique course of each single profile. The registered data show depth-dependent amplitudes along the length of the

Table 2 Technical specifications of the GPR system

Method	**Ground Penetrating Radar (GPR)**
System	GSSI SIR-3000
Sensors	GSSI 270 MHz antenna, model no. 5104A
Measurement Category	Two-way transit time and amplitude of reflected electromagnetic waves
Configuration	Single antenna with survey wheel
Resolution	25 cm profile distance, 2.5 cm point distance
Distance Measurement	GSSI odometer
Data Processing	2D filters (stacking, background removal) and gain functions (AGC) using REFLEXW (Sandmeier Scientific, Germany)
Data Format	Raw data: DZT, processed data: REFLEXW format, time slices: ASCII and GeoTIFF
Image Resolution	0.05 m × 0.05 m

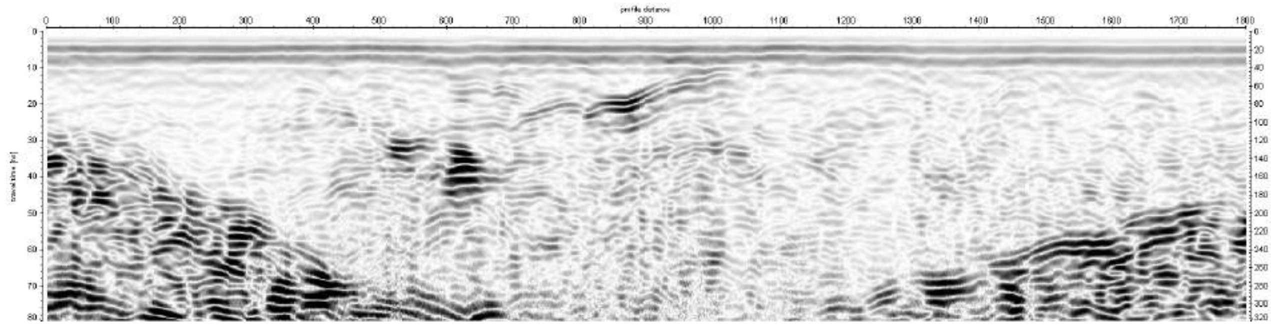

14

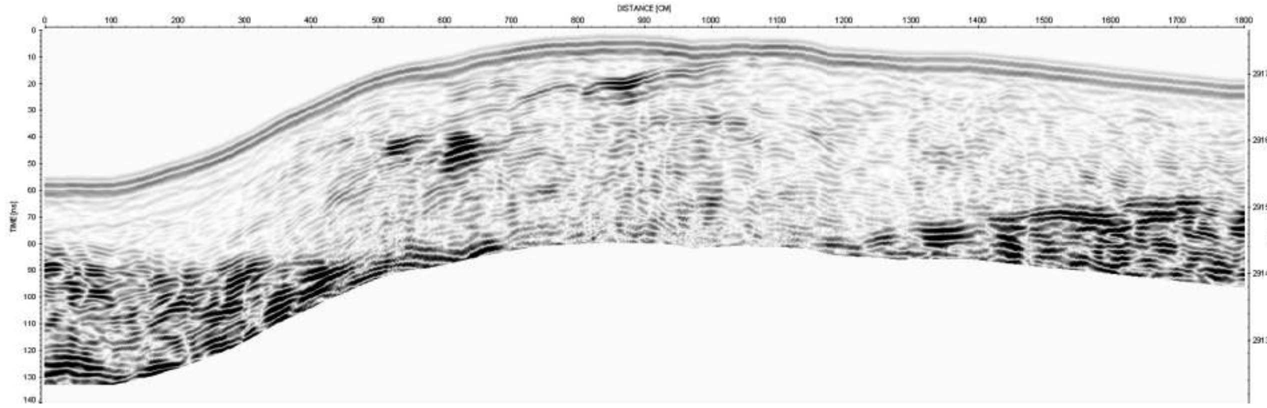

15

Fig. 14 Example of GPR raw data collected along a profile length of 18 m at Mound M3

Fig. 15 The profile from figure 14 corrected to topography

Fig. 16 Scheme of resistivity measurements in the Wenner α configuration on top of a layered half-space (after Knödel et al. 1997, p. 123)

profiles, which have been recorded by the survey wheel (fig. 14). A topographic correction based on available site topography data may show slightly different positions of internal reflection signals, while the depth below the surface is related to the registered time and the electromagnetic wave velocity and is therefore constant (fig. 15).

This example of GPR data shows high reflection amplitudes at the edges of the profile related to the passage from the soil to the bedrock. After topographic corrections were made, it became clear that this layer is a sloped plane towards the hillside. Inside the mound, several high reflection areas related to stone features are probably visible at a depth ranging from between 0.6 m and 1.6 m below the surface.

Electrical Resistivity Tomography (ERT)

Subsurface structures can be detected through electrical resistivity tests if a measurable contrast exists between the resistivity of the target and that of its surroundings. Mainly solid materials, such as stone walls and foundations or solid rock, e.g., bedrock, can be visualized since they maintain a higher resistivity compared to the lower resistivity of loose materials with a higher pore volume, such as with the backfill of ditches and pits. Under average natural conditions, the pore space is saturated or partly saturated, contributing significantly to the electrical conductivity of the ground. This means that daily and seasonal variations could have a strong influence on the resistivity distribution of structures near to the surface. Furthermore, the measurement of the bulk resistivity depends on this electrical conductivity of minerals in a solid phase. A minor amount of clay minerals in a solid phase can considerably increase the conductivity.

For the resistivity measurements, an electric current I is generated into the ground between two electrodes A and B. At the surface the potential difference ΔU of the resulting electrical field is measured between two other electrodes M and N (fig. 16). Depending on the measured parameters – current I and voltage U as well as the positions of the four active electrodes – the derived resistivity is the apparent resistivity for a homogenous section of the ground. The resistivity distribution for the naturally inhomogeneous ground, e.g., when layered, as shown in figure 18, has to be calculated by an inversion process.

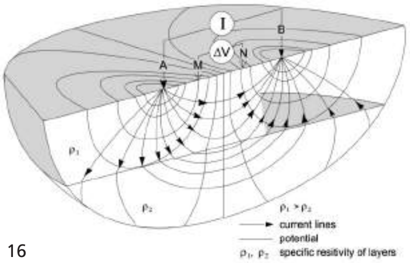

16

For the ERT surveys at Phobjikha, the multi-electrode resistivity meter 4Point Light (Lippmann) with forty electrodes was used. The resistivity measurements were provided along parallel profiles with electrode distances according to the specific survey conditions at the mounds (fig. 17). The technical details of the ERT surveys in the Phobjikha Valley are given in table 3.

For the data inversion we used the software package Boundless Electrical Resistivity Tomography (Rücker et al. 2006). The three-dimensional models of the resistivity distribution were calculated with regard to the topography of the mounds. The topography data were generated from GNSS and theodolite measurements. The modelled resistivity distribution is presented in cross-sections and horizontal slices. In general, the resistivity data show very high resistivity values due to the specific survey conditions characterized by very dry soils and bedrock formation.

3.3 Topographical Survey with GNSS

The positioning of the geophysical data was realized by using a DGPS comprised of two L1 GNSS receivers NovAtel SMART as base and rover (figs. 18 and 19). The relative accuracy with GNSS results in measurements of ± 2 cm. The GNSS device was used for the measurements of the following point and track coordinates:

- Pegs set out in the field to mark the corners of the GPR areas of the six surveyed mounds
- Positions of the electrodes along the ERT profiles at Mounds M1, M3, and M31
- Fixed Points No. 0013971, No. 0017657, and No. 0017688 marked by red plastic cubes near the top of Mounds M1, M3, and M36, respectively (fig. 20)
- Points to map the topography of M31
- Location of Mounds M37, M38, M39, M40, and M41
- Tracks along stones, visible at the surface of Mound M1

The GNSS surveys at Phobjikha Valley were provided in WGS84, UTM Zone 46 projection. Afterwards the coordinates of the three fixed points that had been used became available in the DRUKEREF 03, Wangdue Phodrang TM projection. All geodata were re-projected to DRUKREF 03, Wangdue Phodrang TM projection (EPSG code: 5309). The overall accuracy of the positioning data amounts to ± 2 cm.

3.4 Site Topography Survey with Theodolite

Topographic surveys with a theodolite were performed at Mounds M1, M3, and M31. The point data were referenced to the measured GNSS coordinates and at the end of the campaign exported to standard formats (CAD, ASCII). Afterwards the data were re-projected to DRUKREF 03, Wangdue Phodrang TM projection (EPSG code: 5309). The data are used to generate digital terrain models (DTM) for the covered mounds.

Table 3 Technical specifications of the ERT system

Method	**Electrical Resistivity Tomography (ERT)**
System	4Point Light (multi-channel resistivity meter)
Electrodes	Stainless steel electrodes
Measurement Category	Potential of electrical field ΔU, electrical current I
Configuration	Wenner-α configuration
Resolution	Electrode distance: 0.50–0.75 m
Distance Measurement	Measuring tapes
Topography Measurement	GPS survey of electrode positions; additional topography points using theodolite
Data Processing	BERT (Boundless Electrical Resistivity Tomography)
Data Format	Raw data: ASCII, processed data: VTK output: slices: GRD and GeoTIFF

Fig. 17 ERT surveys at Mound M3. During measurements at the left profile, the right profile was built up.

Fig. 18 GNSS base antenna in the south-eastern area

Fig. 19 Measurements with the GNSS rover at Mound M3

Fig. 20 Fixed point No. 0013971 near the top of Mound M1

The DTM data are plotted onto the geophysical data as contour lines at 0.25 m intervals. Furthermore, the DTM data are used for the modelling of the resistivity distribution with respect to the topography.

3.5 Results and Interpretation

The geophysical surveys in the Phobjikha Valley where carried out at the six selected Mounds M1, M3, M31, M34, M36, and M49. They revealed the following results.

Due to the application of the two geophysical survey methods Ground Penetrating Radar (GPR) and Electrical Resistivity Tomography (ERT), we were able to get complementary images of subsurface structures. The GPR survey provides high-resolution data for shallow and medium depths up to about 3 m. From the ERT surveys along large sections, we were able to gain information at twice the depth of the GPR survey but with lower resolution. The conditions at the end of the dry season were very favourable for the GPR surveys.

The GPR data at the stand-alone Mound M1 (fig. 21) give no hints as to structures related to burials inside the mound down to a depth of 3 m below the surface. The topography surveys point to a rectangular shape of the mound. The arrangement of the stones at the surface points to stair-like constructions. Their continuation inside the mound can be confirmed by small-scale anomalies of enhanced resistivity. The ERT cross-section points to infill that is probably related to the construction of a platform on the eastern slope of the mound.

17

18

19

20

Inside Mound M3, two separate indications with a diameter of about 1 m are derived from the GPR data in the eastern half of the mound. These indications expand from a shallow depth up to a depth of 2 m. The ERT data point to a north/north-west–south/south-east oriented substructure inside Mound M3 (fig. 22). A sloped basement layer below the mound can be derived from both the GPR and ERT data.

The GPR data from the capped Mound M31 show a notable X-shaped substructure with two branches detected over a length of 5 m and 6 m, respectively, at a depth of approximately 1 m (fig. 23). They may point to the central axes of a rectangular basement, confirmed by the ERT data. Various indications at a depth extending between 1.6 and 2.8 m below the surface may point to burial structures.

The data from Mound M34, which is the central mound in a row of three, show a square substructure measuring 5 by 5 m and oriented south-east–north-west and perpendicularly at a depth between 1.0 and 1.8 m below the surface (fig. 24). From 1.8 m to 2.8 m several indications of possibly associated structures are marked. They are slightly displaced towards the south-west with respect to the square substructure.

The data from Mound M36 show square features near the surface (fig. 25). On top of Mound M36, a 2 by 2 m platform can be expected, while a few meters further north, another platform at a level 1 m lower is indicated by a linear anomaly. The square features can be observed up to a depth of 1 m below the surface. With increasing depth, several single indications up to a depth of 3.2 m are clearly recognizable.

The GPR survey at the large capped Mound M49 show no traces of any inner structures which we could identify as a specific feature at the moment. Instead the sloped basement layer can be derived from the data, which means that any indications of stones or constructions would have been detectable if they existed inside the mound.

4. The Archaeological Investigation of Mound M31 in Autumn 2018

During the Geophysical Surveys in spring 2018 Mound M31 attracted attention not only because of its X-shaped interior substructure, but also because of a pit that was observed at the foot of the mound. According to local farmers, soil had been removed

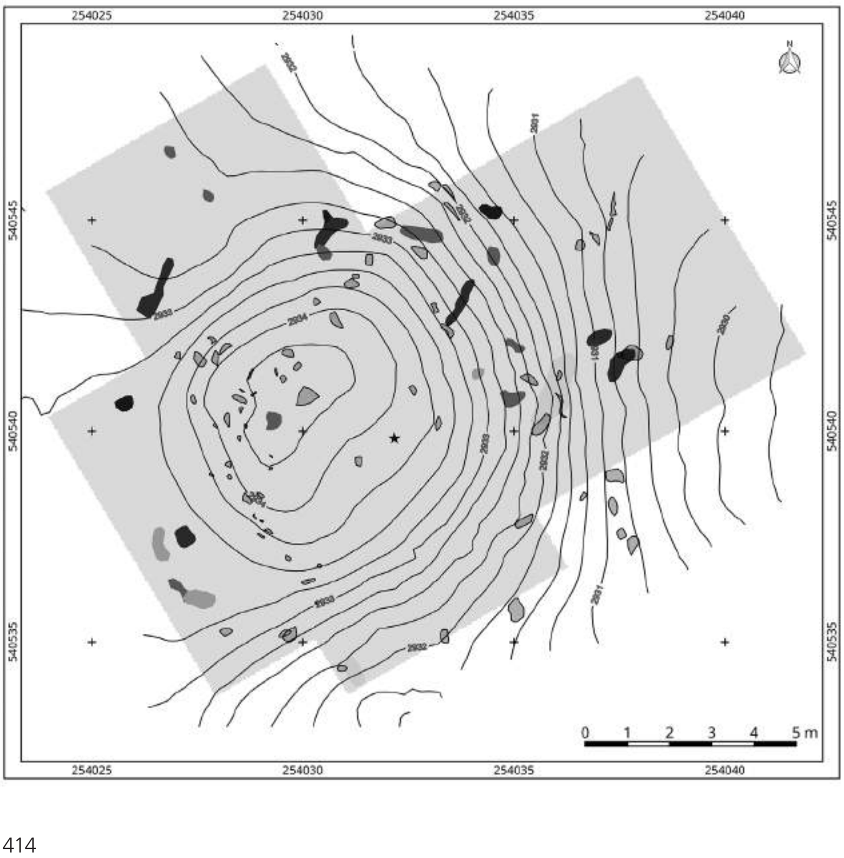

Fig. 21 GPR interpretation up to 1.0 m of Mound M1; the arrangement of the stones at the surface points to stair-like constructions Contour lines: 0.25 m (Eastern Atlas, Burkart Ullrich)

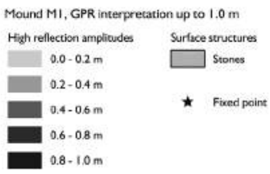

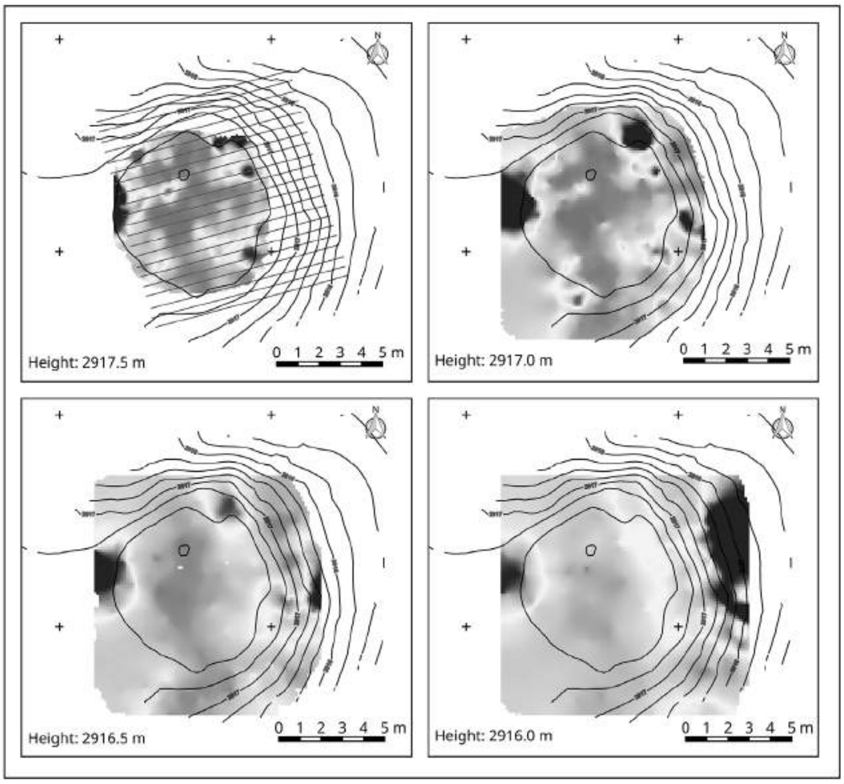

Fig. 22 ERT data of Mound M3, pointing towards a north/north-west–south/south-east oriented substructure inside the mound Contour lines: 0.25 m (Eastern Atlas, Burkart Ullrich)

Mound M3, ERT data
Horizontal slices of 3d-model at selected heights

Electrical resistivity

Resistivity profiles

Electrode distance: 0.5 m

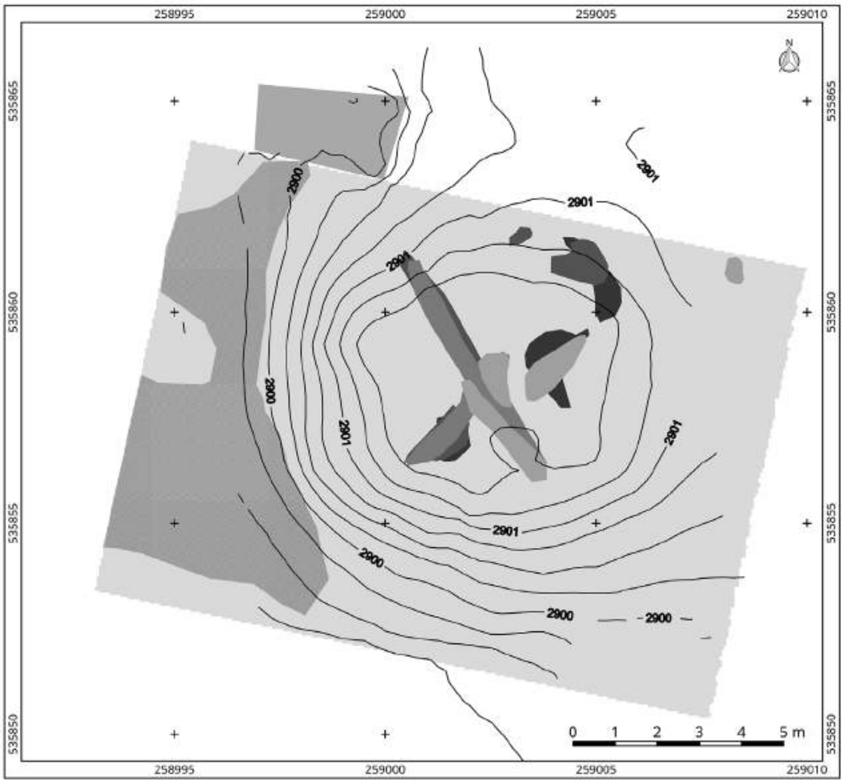

Fig. 23 GPR interpretation 0.8 to 1.6 m of Mound M31, showing an X-shaped substructure Contour lines: 0.25 cm (Eastern Atlas, Burkart Ullrich)

Mound M31, GPR interpretation 0.8 to 1.6 m

High reflection amplitudes
0.8 - 1.0 m
1.0 - 1.2 m
1.2 - 1.4 m
1.4 - 1.6 m

Related to
Rock
Trench S1

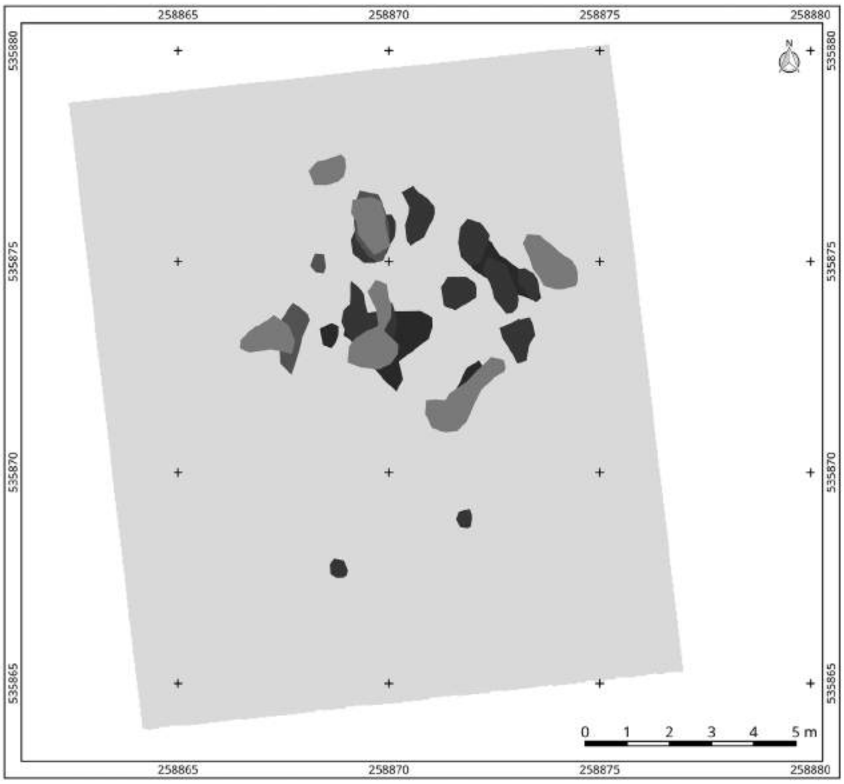

Fig. 24 GPR interpretation 1.0 to 1.8 m of Mound M34, with a square substructure (Eastern Atlas, Burkart Ullrich)

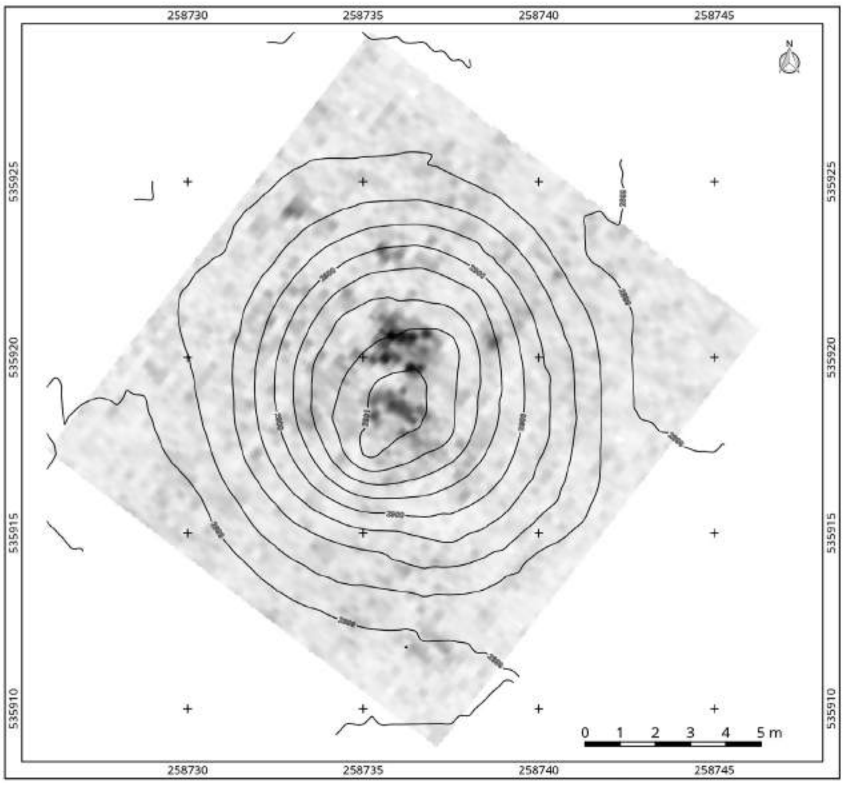

Fig. 25 GPR data of Mound M36, showing two square features near the surface Contour lines: 0.25 cm (Eastern Atlas, Burkart Ullrich)

Fig. 26 Southern profile of the soil removal pit at Mound 31

1 natural substrate
2 burnt-black layer with ^{14}C dating to fifth/sixth century
3 mound fill layer
4 recent humus grid space 1 meter

Fig. 27 Overview of the X-shaped tunnel structure

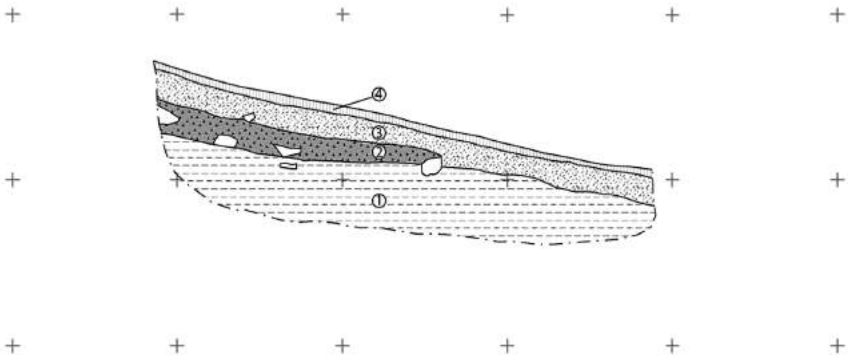

26

during repair work done on the road (fig. 11). Since the pit had cut through the mound, we decided to clean up the southern longitudinal profile and document it with drawings and photographs (fig. 26). In fact, in this profile we were able to grasp the structure of the layers of the artificially piled-up mound at its periphery: above the original natural surface was a black layer of burnt material, which here constituted the lowest layer of the mound. On top of this came a deposit of earth material from the immediate surroundings, upon which a thin layer of humus had formed. A charcoal sample could be retrieved from the burnt layer. Using the radiocarbon method, it was dated as stemming from 426–558 AD.

The unique X-shaped structure and its dating to the fifth or sixth century led to the decision to investigate Mound M31 as part of an archaeological excavation. This took place from 5 October to 5 November, 2018. Under the co-direction of Christian Bader and Karma Tenzin and with the support of master's students Benjamin Hart and Alexander Keiser of the University of Zurich, the following DCHS staff members completed the excavation work: Shacha Gyeltsen, Sonam Gyeltsen, Sonam Tenzin, Tenzin Wangchuk, Pema Wangda, and Tashi Dawa.

To obtain complete profiles at right angles to each other, the mound was quartered with a crosscut in such a way that in each of the four sectors one of the arms of the X-structure observed in the GPR survey images was expected to be located. All sectors were removed by hand in slices of about 20 cm down to the naturally outcropping substrate. Proceeding in this way, the X-shaped structure recognizable in the GPR survey images could be completely exposed and documented (figs. 27–30). What emerged was a canal-like structure of parallel, perpendicular stone slabs, which were covered by

27

Fig. 28 Intersection point of the X-shaped tunnel structure with slab covers lifted

Fig. 29 Tunnel structure resting on the lowest black layer

Fig. 30 Stepped walls with tunnel mouth in the centre of the middle step

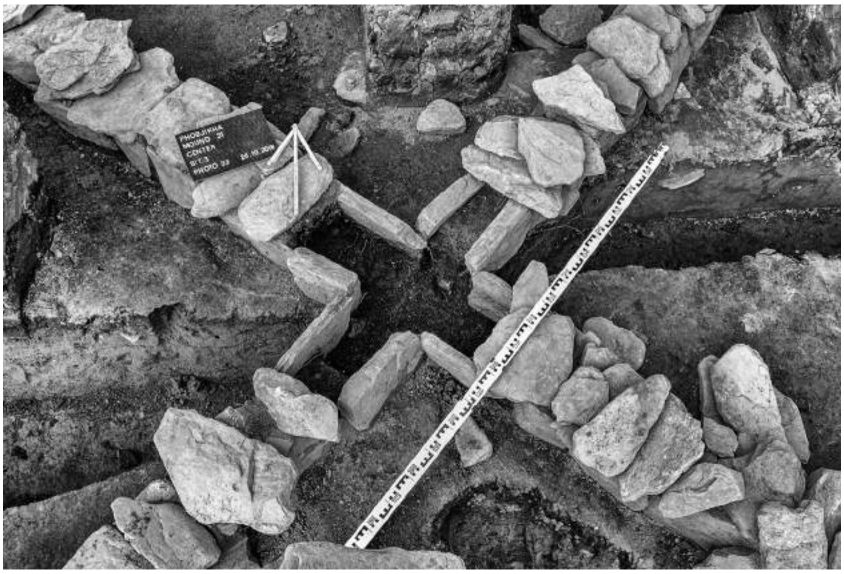

28

29

30

Fig. 31 Small glass beads from the intersection point of the X-shaped tunnel structure

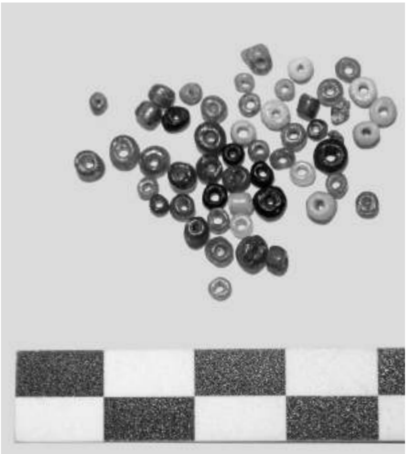

31

stones that were also flat. At the intersection point of the X-structure, the slab covers were lifted up and the material inside of the canal was carefully removed. This fill was identical to the material of the mound fill. Directly under the slab covers a few small, differently coloured glass beads surfaced (fig. 31).

On the north-west side of the mound, three parallel, stepped drystone walls were uncovered; these had not been recognizable in the GPR surveys that were performed in the same direction. The steps were partially preserved up to three risers. At the centre of the middle step was the mouth of one of the tunnel arms (fig. 30). Remains of drystone walls also appeared in the north-east sector. Unfortunately only a few stones were preserved. However, these were sufficient to postulate a stair situation analogous to the one in the adjacent north-west sector. Further, this finding implied that stones had been removed in the past. There were no signs of drystone walls in the southern sectors, a finding that could also be due to stone removal.

On the basis of the documented profiles, the structure of the mound could be well observed. An initial fill of light-brown clay lay over the naturally occurring soil, followed by a black, clayey-humus layer with little charcoal. This black layer constituted the construction horizon of the canal structure, and is to be correlated with the ^{14}C dating of the black layer from the pit profile completed during the project in spring 2018. A heterogeneous layer of fill could be seen on top of the black layer, which was in turn overlaid by strata of black, clayey-humus lenses. The uppermost black lenses lay at the height of the stone covers of the canal structure. This was followed by only a homogeneous mound fill of redistributed material from the surroundings, and lastly, by recent humus.

Apart from a few ceramic fragments, which mainly originated from the uppermost mound fill and the humus, hardly any finds surfaced. In addition to two small iron objects (possibly the cutting edge of a knife and a nail or bullet) and the glass beads, some charcoal samples for ^{14}C dating could be retrieved from the black layers.

No indices of a burial appeared; neither ash fill with cremation remains nor burial objects could be found. The interpretation of Mound M31 and its X-shaped tunnel will be dealt with in a master's thesis currently being carried out by Benjamin Hart in the Department of Prehistoric Archaeology, University of Zurich.

5. Outlook

Taking into account the special circumstances of this investigation, i.e., that it is the first of its kind in Bhutan, no examples comparable to our findings currently exist. However, there are other mounds (M1, M34, and M36) that according to the GPR survey results also appear to be rectangular-shaped and possibly have stepped walls. An archaeological investigation of one of these mounds should be considered to extend the database. Other possible objects of investigation are Mounds M44, M45, and M46 in the farmland near the village called Kilkhorthang in Phobji Gewog. The existence of these three mounds is endangered because ploughing by local farmers has already damaged them.

Bibliography

DELLA CASA, PH., FUX, P., NAGTSHO DORJI, KARMA TENZIN, SANGAY KINGA, TENZIN WANGCHUK, NAMGYEL TSHERING, BADER, CH., 2015: *The Bhutan-Swiss Archaeology Project* 2014*: strengthening institutional structures and scientific cooperations*. In SLSA: Annual report 2014. Zurich, p. 167–170.

FUX, P., WALSER, CH., NAMGYEL TSHERING, 2014: *Archaeology in the Kingdom of Bhutan: Exploring the Country's Prehistory*. In SLSA: Annual report 2013. Zurich, p. 29–40.

JOL, H.M., 2009: *Ground Penetrating Radar: Theory and Applications*. Amsterdam and Oxford: Elsevier.

KNÖDEL, K., KRUMMEL, H., LANGE, G. (Hrsg.), 1997: *Handbuch zur Erkundung des Untergrundes von Deponien und Altlasten. Band 3: Geophysik*. Berlin: Springer.

RÜCKER, C., GÜNTHER, T., SPITZER, K., 2006: *Three-dimensional modelling and inversion of dc resistivity data incorporating topography – I. Modelling*. Geophysical Journal International 166.2, p. 495–505.